A deep sub-wavelength process for the formation of highly uniform arrays of nanoholes and nanopillars

To cite this article: Wei Wu *et al* 2007 *Nanotechnology* **18** 485302

View the article online for updates and enhancements.

Related content

- The fabrication of high-aspect-ratio, size-tunable nanopore arrays by modified nanospherelithography
X Chen, X Wei and K Jiang

- Fabrication of nanopillars by nanosphere lithography
C L Cheung, R J Nikoli, C E Reinhardt et al.

- Fabrication of metal nanoparticle arrays by controlled decomposition of polymer particles
D Brodoceanu, C Fang, N H Voelcker et al.

Recent citations

- Photonic Jet Writing of Quantum Dots Self Aligned to Dielectric Microspheres
Andrea Ristori *et al*

- Recent progress in surface plasmon resonance based sensors: A comprehensive review
Vasimalla Yesudasu *et al*

- Nanopatterning with Photonic Nanojets: Review and Perspectives in Biomedical Research
Salvatore Surdo *et al*

A deep sub-wavelength process for the formation of highly uniform arrays of nanoholes and nanopillars

Wei Wu, Alex Katsnelson, Omer G Memis and Hooman Mohseni

EECS Department, Northwestern University, Evanston, IL 60208, USA

E-mail: hmohseni@ece.northwestern.edu

Abstract
We report a low-cost and high-throughput process for the realization of two-dimensional arrays of deep sub-wavelength features using silica and polystyrene spheres. The pattern size in this method is a weak function of sphere size, and hence excellent size uniformity is achievable. Also, the period and diameter of the holes and pillars formed with this technique can be controlled precisely and independently. Moreover, the patterns can be formed in conventional negative and positive photoresists, and hence this approach is compatible with a wide range of existing processing methods. Although we achieved hole sizes of ∼250 nm with a broadband UV source centered at 400 nm, our simulation results show that patterns as small as 180 nm should be achievable at a wavelength of 365 nm.

(Some figures in this article are in colour only in the electronic version)

1. Introduction

There is an increasing demand for high-throughput and parallel nanofabrication techniques. In particular, there is a high demand for a low-cost process capable of producing highly uniform arrays of nanopillars and nanoholes, since these patterns have found a wide range of applications in many devices such as solar cells [1], photodetectors [2], surface plasmonics [3], photonic crystals [4], memory devices [5], nanofiltration [6], fuel cells [7] and artificial kidneys [8]. Conventional photolithography techniques cannot satisfy the small dimension requirements in many of these applications, due to the light source's wavelength limit [9]. Novel techniques such as x-ray [10], electron-beam [11], focused ion beam [12] and nanoimprint [13] lithography can achieve the desired resolution, but are either too slow or expensive for fabrication over large areas. Nanosphere lithography (NSL) [14–17] is a promising approach that uses planar ordered arrays of micro/nanospheres as a lithography mask to generate ordered nanoscale arrays on the substrate. However, there are several limitations associated with this method. First is that the monolayer of spheres can always contain dislocations resulting in agglomerations of particles after metal evaporation and prevent successful lift-off [5]. Second, the size and spacing of the holes are coupled, and hence these properties cannot be independently controlled [18]. Finally, NSL requires spheres to be formed directly on the substrate surface [14], which is not possible for many materials.

Here we present a novel photolithography technique, utilizing the self-assembled planar array of spheres as optical lenses to generate deep sub-wavelength regular patterns over large areas on a photoresist. Previous studies showed that spheres with correct optical index values can focus light into deep sub-wavelength dimensions [19]. We noticed that both silica and polystyrene (PS) have optical indices [20] that are close to the optimum value at the wavelengths used by conventional UV lithography. Interestingly, our full three-dimensional finite difference time domain (3D-FDTD) calculations show that the beam waist is a very weak function of the sphere diameters and hence an extremely uniform pattern size can be achieved even for relatively poor sphere size uniformity. Figure 1 shows our simulation results for conventional UV lithography i-line (wavelength = 365 nm) and silica spheres of sizes from 0.5 to 5 μm. Using a linear fit, the relation between the sphere diameter d and FWHM (full width at half-maximum) w of the focused light is found to be $w = 0.0056d + 160$ (nm). This means that the variation of the FWHM of the focused light is about 0.6% of the change in
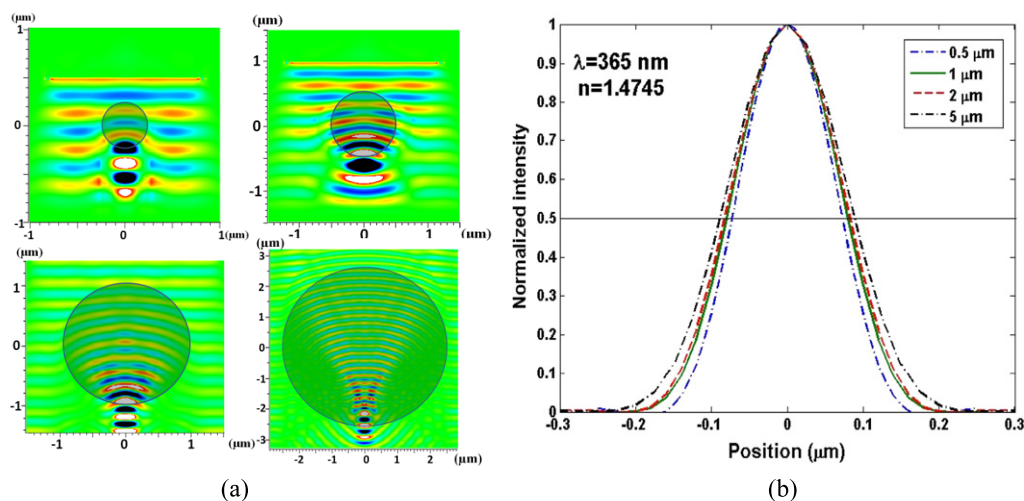
Figure 1. (a) 3D-FDTD simulations of the electrical field profile for silica micro/nanospheres with diameters of $D = 0.5, 1, 2$ and 5 μm at $\lambda = 365$ nm. (b) The normalized light intensity cross section shows a very small change of the beam FWHM despite a 10-time change in the sphere diameter.
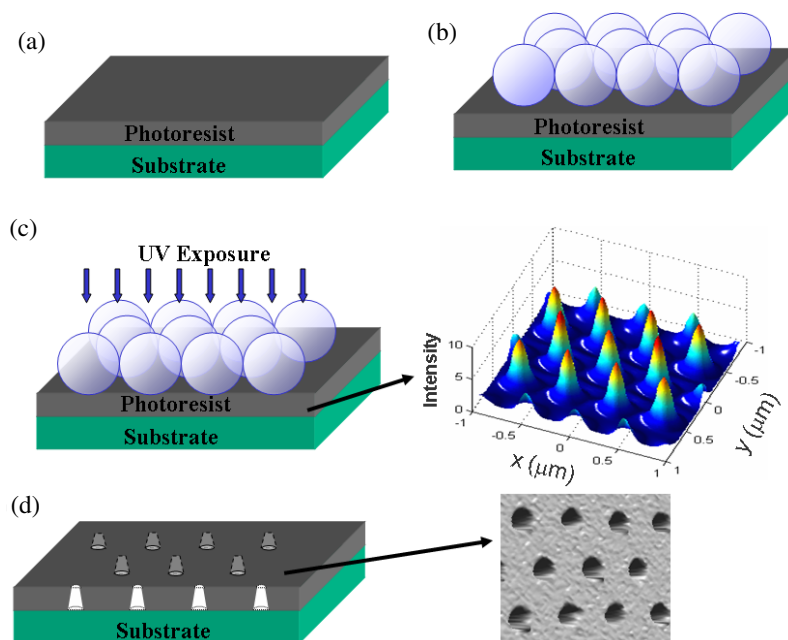

Figure 2. A schematic illustration of the process for the fabrication of periodic nano-arrays: (a) spin-on deposition of photoresist on a substrate, (b) a monolayer of silica or PS spheres formed on top of the photoresist, (c) UV light exposure of the photoresist covered by the monolayer of HCP microspheres. The two-dimensional intensity of the UV light in the photoresist plane, calculated by our three-dimensional FDTD, is shown on the right, (d) sub-wavelength patterns obtained after removing the spheres' photoresist development. An AFM image of a developed photoresist is shown on the right.

the sphere's diameter. Similar simulation results could also be obtained for polystyrene spheres. FWHM is a good measure of the photoresist exposure, since the etching rate usually changes by almost an order of magnitude for a 50% optical intensity change around the photoresist threshold dose [21].

2. Experimental details

We prepared GaAs substrates with two kinds of commonly used photoresists (PR), AZ 5214-E and Shipley 1805. All

process steps were performed in a class 100 clean-room. Two types of spheres, silica and PS, were used to form hexagonal close packing (HCP) arrays on top of the photoresists. We used 10 wt% aqueous suspension of transparent silica or polystyrene spheres of 0.97 μm diameter. Before usage, the aqueous suspension was diluted by DI water down to 0.1 wt% for both types of spheres. A higher concentration of the spheres forms multilayers of spheres and a low concentration would not be enough to form a complete layer. The fabrication process is schematically illustrated in figure 2. Both photoresists were
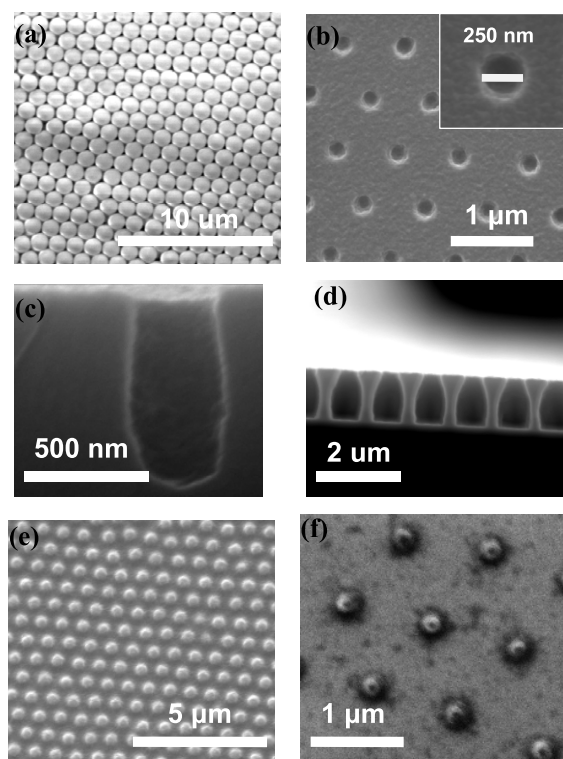
Figure 3. SEM images of (a) a single layer of microspheres (0.97 μm diameter) deposited on top of the photoresist; (b) AZ5214 nanoholes (inset is a more enlarged image), after sphere removal and photoresist developing; (c) a cross section of nanopatterns formed by silica spheres and AZ5214 photoresist, (d) a cross section of nanopatterns formed by silica spheres and AZ5214 photoresist, (e) AZ5214 photoresist used as negative photoresist and formed nanopillars; (f) Shipley 1805 photoresist used as negative photoresist.

spun onto GaAs substrates at 5000 rpm for 1 min, and soft baked for 90 s at 90 °C. After soft bake, the photoresist-covered samples were dipped into AZ-300 MIF developer

solution for a few seconds. This step made the photoresist surface hydrophilic enough to promote formation of a monolayer of HCP silica or PS spheres directly on top of the photoresist. To form a good monolayer, we carefully studied the effects of different concentrations of the spheres, the amount of the sphere suspensions added, the evaporation rates of water and different tilt angles. Next, the samples were UV exposed using a conventional photolithography tool (Quintel Q-4000) at a lamp power of about 11.4 mW cm^{-2} and center wavelength of 400 nm for about 0.8 s. The short time was not enough to expose the photoresist except at the focused areas. Silica spheres were removed by dipping the sample into hydrofluoric acid for 30 s, while sonication was used to remove PS spheres. Photoresists were developed in AZ-300 MIF developer for about 30 s, rinsed by DI water and dried by nitrogen.

3. Results and discussion

Figure 3(a) shows the SEM image of a typical monolayer of silica spheres with $d \sim 0.97$ μm formed on top of the photoresist. Figure 3(b) shows the top view of SEM images of the developed samples. The minimum diameter of the hole is about 250 nm. The ratio of the feature size to the wavelength used is about 0.625. The hole lattice has a periodicity of 0.97 μm, almost identical to the diameter of the spheres. Figures 3(c) is the cross-sectional image of a hole in the AZ5214 photoresist. It shows a high aspect ratio, which can be utilized for demanding lift-off and deep dry etching processes. The process could be modified to produce holes with negative sidewall slopes for a more aggressive lift-off process (see figure 3(d)). We could also form pillars of photoresist using negative resist processing. To use AZ5214 photoresist as a negative photoresist, we post-baked the photoresist at 120 °C for 180 s, followed by 2 min of post-exposure. Also, we converted Shipley 1805 to negative photoresist by inserting the samples into an ammonia environment at 90 °C for 1 h, followed by a post-exposure step for about 2 min. Figure 3(e)
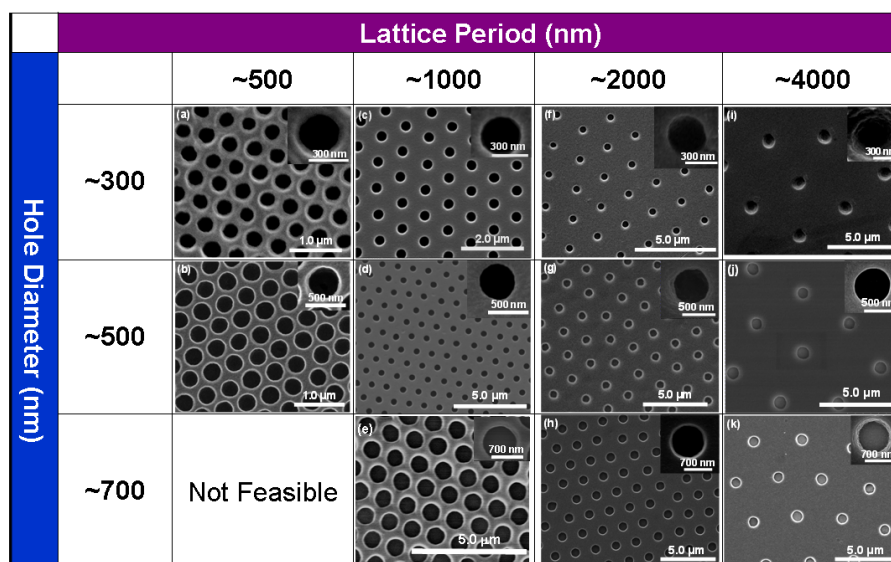
Figure 4. SEM images of uniform two-dimensional HCP lattices of nanoholes with different hole diameter and lattice period.
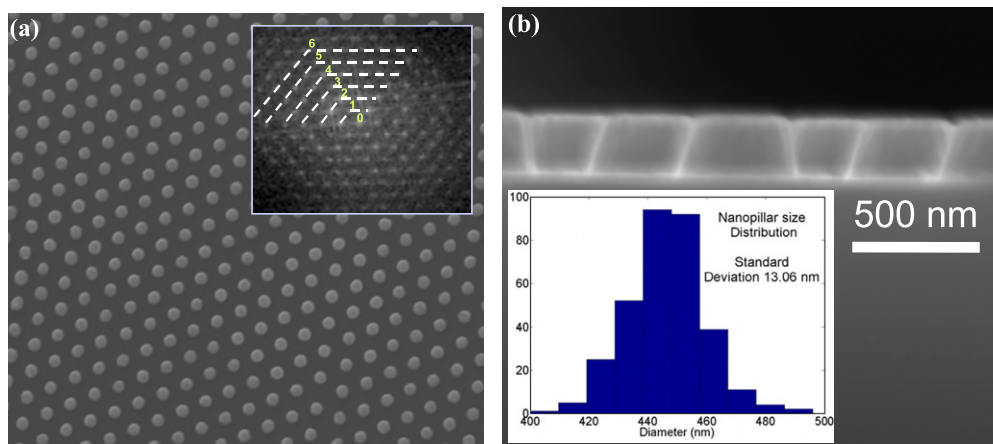
Figure 5. (a) SEM top image of HCP arrays of gold nanopillars. The inset shows the 2D Fourier transform, demonstrating the excellent coherence of the pillars' position and size. (b) High-resolution side view SEM image of the gold nanopillars. The inset shows the nanopillar size distribution, which is currently limited by our image resolution.

shows the top view of the AZ5214 photoresist pillars, while figure 3(f) shows the top view of the Shipley 1805 photoresist pillars.

We could change the sizes of the holes, as well as the hole-to-hole distance in the arrays precisely and independently. Figure 4 shows an example of such flexibility with uniform HCP arrays of holes with hole diameters of about 300, 500 and 700 nm with lattice periods of about 500, 1000, 2000 and 4000 nm. The hole diameter could be controlled with varying exposure time, and the hole-to-hole distance (lattice period) was controlled by different spherical diameters. Obviously, an array of holes with a lattice period smaller than the hole diameter is not feasible (e.g. 700 nm holes with a 500 nm period).

Figure 5(a) shows an example of HCP arrays of gold nanopillars resulting from the lift-off process. The inset shows a 2D Fourier transform of the SEM image of the nanopillars. The Fourier image shows narrow hexagonal patterns up to high satellite orders, due to a highly coherent structure. Such coherence is particularly important for the photonic crystal applications. Figure 5(b) shows the magnified side view of the gold pillars. The inset shows the histogram size distribution, showing a standard deviation of about 13 nm in diameter. Unfortunately, this value is limited by our image digitization resolution with ~15 nm per pixel. Higher magnification images show much smaller standard deviation values, while the number of pillars in those images is not statistically large enough.

4. Summary

In conclusion, we have demonstrated a novel maskless sub-wavelength photolithography technique with a potentially high throughput for the formation of HCP arrays of deep sub-wavelength holes and pillars. This method provides accurate and independent control of the hole's diameter and the lattice period. Using a broadband UV source, we demonstrated highly uniform features that are about 0.6 times the exposure wavelength, while theoretical calculation predicts feature sizes that are about half, for a narrow line UV source down to a wavelength = 193 nm.

References

[1] Chiu W L, Alkaisi M M, Kumaravelu G, Blaikie R J, Reeves R J and Bittar A 2006 *Adv. Sci. Technol.* **51** 115–20
[2] Rogalski A 2003 *J. Appl. Phys.* **93** 4355–91
[3] Dintinger J, Klein S and Ebbesen T W 2006 *Adv. Mater.* **18** 1267–70
[4] Masuda H, Ohya M and Nishio K 2000 *J. Appl. Phys.* **39** 1039–41
[5] Weekes S M, Ogrin F Y and Murray W A 2004 *Langmuir* **20** 11208–12
[6] Baker R W 2004 *Membrane Technology and Applications* 2nd edn (Chichester: Wiley)
[7] Shah K, Shin W C and Besser R S 2003 *J. Power Sources* **123** 172–81
[8] Gadegaard N, Martines E, Riehle M O, Seunarine K and Wilkinson D W 2006 *Microelectron. Eng.* **83** 1577–81
[9] Martin O J F 2003 *Microelectron. Eng.* **67-8** 24–30
[10] Silverman J P 1997 *J. Vac. Sci. Technol.* B **15** 2117–24
[11] Corbierre M K, Beerens J and Lennox R B 2005 *Chem. Mater.* **17** 5774–9
[12] Melngailis J, Mondelli A A, Berry I L and Mohondro R 1998 *J. Vac. Sci. Technol.* B **16** 927–57
[13] Chou S Y, Krauss P R and Renstrom P J 1996 *J. Vac. Sci. Technol.* B **14** 4129–33
[14] Zhang X Y, Whitney A V, Zhao J, Hicks E M and Van Duyne R P 2006 *J. Nanosci. Nanotechnol.* **6** 1920–34
[15] Whitney A V, Myers B D and Van Duyne R P 2004 *Nano Lett.* **4** 1507–11
[16] Kosiorek A, Kandulski W, Chudzinski P, Kempa K and Giersig M 2004 *Nano Lett.* **4** 1359–63
[17] Kosiorek A, Kandulski W, Glaczynska H and Giersig M 2005 *Small* **4** 439–44
[18] Vossen D L J, Fific D and Blaaderen A V 2005 *Nano Lett.* **5** 1175–9
[19] Chen Z, Taflove A and Backman V 2004 *Opt. Express* **12** 1214–20
[20] Mal X, Lu J, Brock R, Jacobs K, Yang P and Hu X 2003 *Phys. Med. Biol.* **48** 4165–72
[21] See for example, Shipley 1800 series photoresist development curves at http://cmi.epfl.ch/materials/Data_S1800.pdf